NANO LETTERS

Letter

pubs.acs.org/NanoLett

Personal Thermal Management by Metallic Nanowire-Coated Textile

Po-Chun Hsu,[†] Xiaoge Liu,[‡] Chong Liu,[†] Xing Xie,[§] Hye Ryoung Lee,[∥] Alex J. Welch,[†] Tom Zhao,[†] and Yi Cui*[,†,⊥]

[†]Department of Materials Science and Engineering, [‡]Department of Applied Physics, [§]Department of Civil and Environmental Engineering, and [∥]Department of Electrical Engineering, Stanford University, Stanford, California 94305, United States

[⊥]Stanford Institute for Materials and Energy Sciences, SLAC National Accelerator Laboratory, 2575 Sand Hill Road, Menlo Park, California 94025, United States

Supporting Information

ABSTRACT: Heating consumes large amount of energy and is a primary source of greenhouse gas emission. Although energy-efficient buildings are developing quickly based on improving insulation and design, a large portion of energy continues to be wasted on heating empty space and nonhuman objects. Here, we demonstrate a system of personal thermal management using metallic nanowire-embedded cloth that can reduce this waste. The metallic nanowires form a conductive network that not only is highly thermal insulating because it reflects human body infrared radiation but also allows Joule heating to complement the passive insulation. The breathability and durability of the original cloth is not sacrificed because of the nanowires' porous structure. This nanowire cloth can efficiently warm human bodies and save hundreds of watts per person as compared to traditional indoor heaters.

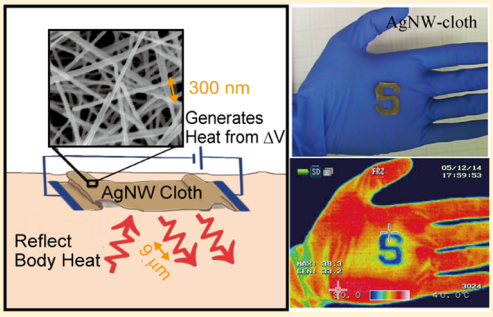

KEYWORDS: *metallic nanowires, textile, low-emissivity materials, thermal management*

One million years ago, early humans first began to use fire to stay warm.[1] Today, we have many more forms and end uses for energy, but 47% of global energy continues to be spent simply on indoor heating, and 42% of that specifically for residential building heating.[2] Considering this enormous portion of energy use, how to mitigate the energy use of heating is critical to solving the global energy crisis. Another equally serious issue—global warming—is also highly connected to the usage of heating. The Intergovernmental Panel on Climate Change (IPCC) showed that human-generated greenhouse gases are responsible for the global surface temperature increase, 0.74 ± 0.18 °C during the past 100 years.[3] Studies have shown that heating contributes up to 33.5% of total greenhouse gas emission,[4,5] which again explains the significant impact of heating on our environment. These statistics explicitly demonstrate the vital role of heating in the world's energy issue. To reduce indoor heating, policy makers usually focus their efforts on elevating the insulation requirements for buildings,[6,7] and many efforts in the scientific community have been made to study building materials with high R-values and low emissivity windows.[8−11] However, there is still a large portion of energy wasted to maintain the temperature of empty space and inanimate objects inside the building rather than focusing on humans. If heating and insulation could be managed directly based on humans, a vast amount of energy could be saved. This optimal energy-saving approach is called "personal thermal management". A personal thermal management device should be wearable just like normal clothes and capable of reducing the loss of body heat or even raising the body's temperature if desired. Here, we demonstrate that solution-processed metallic nanowire mesh can be easily coated onto existing textiles to achieve this concept. Since the demonstration of metallic nanowire synthesis,[12,13] metallic nanowire networks have been widely used for transparent conductors and have become one of the most promising alternative candidates to indium tin oxide transparent conductor.[14−22] The metallic nanowires connect with each other and form a conducting network, and the empty space between neighboring nanowires provides transmittance for visible light. For personal thermal management, the function and the requirement of the dimensions of empty space are somewhat different. Here, the goal is for infrared radiation to be reflected back toward the body to reduce heat loss, so the dimension of the empty space is smaller than the IR wavelength. Metallic nanowire cloth has great potential to reduce the energy used on indoor heating because of its personal thermal management capabilities while retaining the wearability and breathability of normal cloth.

Figure 1a illustrates our simple yet effective method of personal thermal management with a metallic nanowire textile. Normal cloth traps the air surrounding the human body to decrease heat transfer via convection and conduction, but its high emissivity (0.75−0.9) provides little radiative insulation.[23] After coating the cloth with metallic nanowires and forming a

Received: September 23, 2014
Revised: November 12, 2014

ACS Publications © XXXX American Chemical Society

dx.doi.org/10.1021/nl5036572 | *Nano Lett.* XXXX, XXX, XXX−XXX

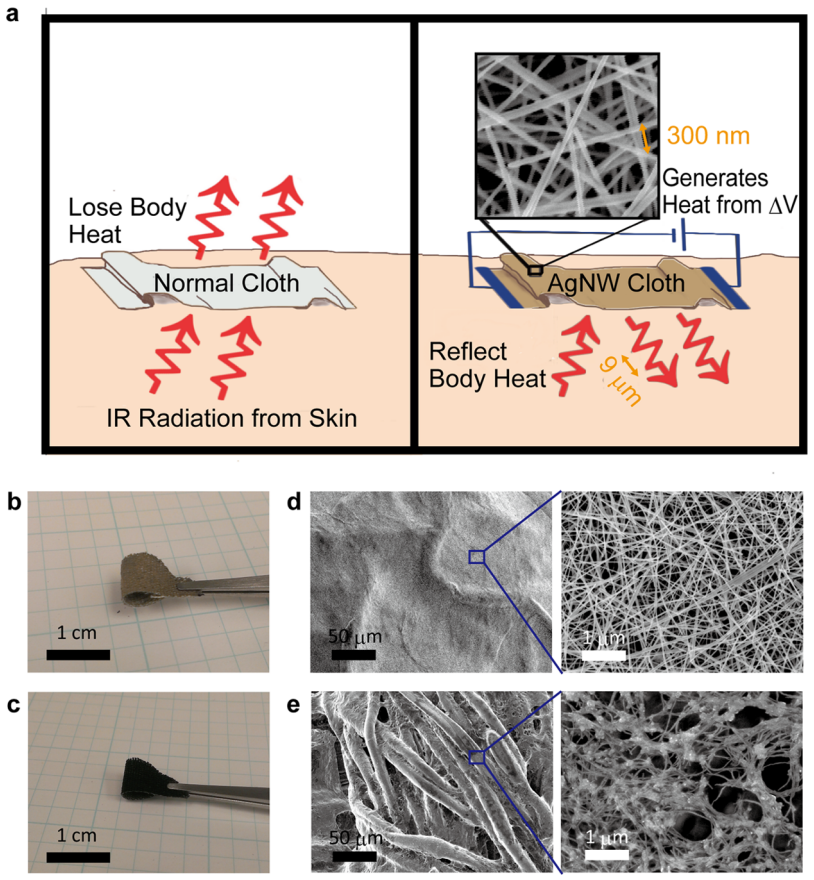

Figure 1. (a) Concept illustration of nanowire cloth with thermal radiation insulation and active heating. (b)(c) Photos of AgNW-cloth and CNT-cloth showing the flexibility of nanowire cloths, respectively. (d) SEM images of AgNW-cloth. Because AgNWs are larger in both diameter and length, the coating is more compact and forms the conductive network. (e) SEM images of CNT-cloth. The coating is more conformal compared to AgNWs.

metallic conducting network, the majority of human body radiation is reflected back toward the body, greatly enhancing the insulation performance. The spacing between nanowires is controlled to be between 200 and 300 nm. Human body radiation is generally 9 μm in wavelength, so most of it "sees" the nanowire cloth as a continuous metal thin film and is reflected. However, unlike a continuous metal film, which is vapor impermeable, the spacing of the metallic nanowire network is much larger than a water molecule. Therefore, water vapor generated by perspiration can easily escape, making the wearer feel comfortable. In addition to reflecting body radiation, if an electricity source is connected to the textile, the low sheet resistance of the metallic nanowire network can provide effective Joule heating to further increase the skin temperature. We use silver nanowires (AgNWs) and carbon nanotubes (CNTs) to realize the personal thermal management cloth concept. Due to the nanoscale dimensions of AgNWs and CNTs, the coated cloth is as flexible as normal cloth, as shown in Figure 1b and c, respectively. In Figure 1d, the scanning electron microscope (SEM) images show that the AgNWs are around 70 nm in diameter and tens of microns in length. Their spacing is approximately 200 nm depending on areal mass loading. The AgNWs form a conductive porous network on the textile, which allows for vapor permeability, IR reflection, and Joule heating capability. On the other hand, in Figure 1e, CNT bundles are approximately 5 nm in diameter and 1 μm in length. The CNT network is conductive and thus suitable for Joule heating, although its emissivity is reported to be 0.98[24] and does not provide IR reflection. Nevertheless, the high chemical stability of CNT still makes it an advantageous material for personal thermal management.[25]

To describe the IR optical properties of AgNW-cloth, the equivalent sheet impedance of the simplified model was applied to simulate the metallic NW network, as illustrated in Figure 2a.[26] A detailed derivation is given in the Supporting Information. In Figure 2b, the reflectance of 200, 400, and 600 nm nanowire spacing is shown versus wavelength from 2 to 30 μm, assuming normal incidence. Human body radiation spectrum is also illustrated for comparison. The three wire mesh spacings are all highly reflective in the majority of the human body radiation spectrum, which peaks at ~9 μm. This shows that metallic nanowire meshes are effective at trapping the thermal radiation around human bodies. To obtain a broader sense of reflectance dependence on wire spacing, the reflectance spectra are weighted by human body radiation to deduce a weighted average reflectance, which is plotted versus a range of nanowire spacings from 100 to 2000 nm, as shown in Figure 2c. In our experiment, the nanowire spacing is approximately 300 nm, which corresponds to ~97% reflectance in the simulation. Even in the case of large spacing at 2000 nm where the mass loading is low, the reflectance is still 50%, which is huge as compared to the low radiation insulation of normal cloth. In practice, however, human body radiation comes from all directions, so the angular dependence should also be investigated as shown in Figure 2d. The nanowire mesh maintains its high reflectance from 0° (normal incidence) to

dx.doi.org/10.1021/nl5036572 | Nano Lett. XXXX, XXX, XXX−XXX

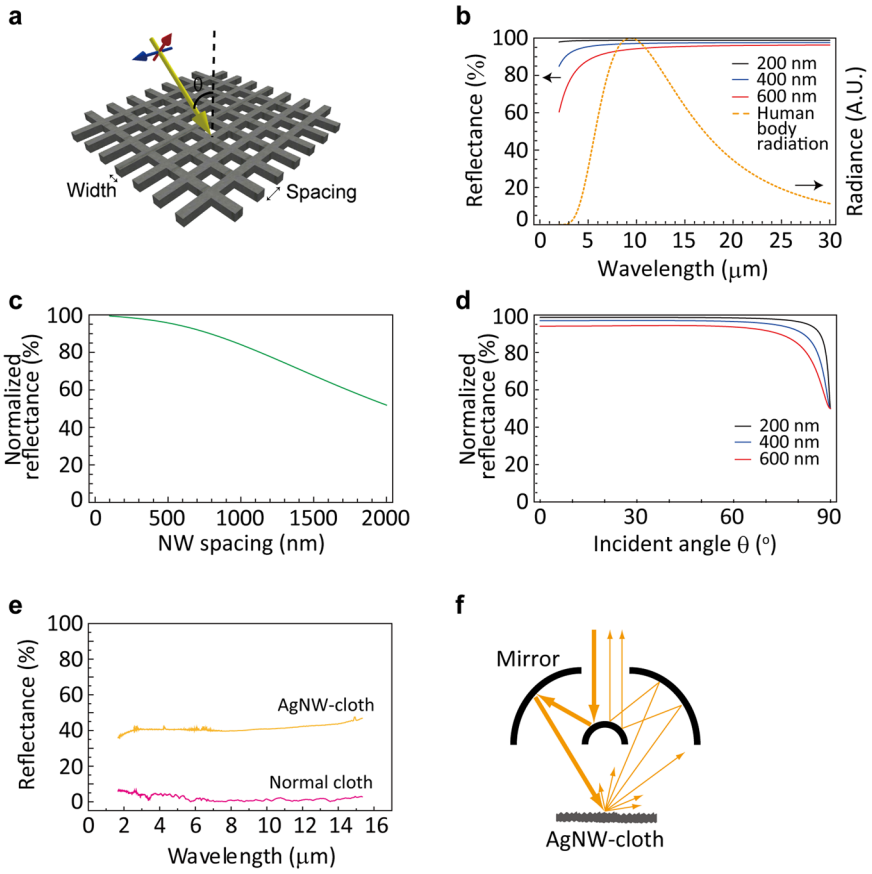

Figure 2. (a) Simulation model for describing the IR reflectance of a metallic NW mesh. (b) Calculated normal-incidence spectral reflectance of nanowire mesh with spacing of 200, 400, and 600 nm. Human body radiation spectrum is also shown to emphasize the dominant wavelength region that the nanowire mesh should reflect. (c) The normalized reflectance weighted by human body radiation as a function of nanowire mesh spacing. The normalization is with respect to the spectral distribution of human body radiation. For typical dip-coated AgNW cloth, the spacing is ~300 nm, which corresponds to 97% of normalized reflectance. (d) Angular dependence of normalized reflectance of different mesh spacings. The normalization is again based on the spectral distribution of human body radiation. The normalized reflectance remains constant for a wide range of incident angles, suggesting that the insulation of nanowire mesh is effective for all-angle radiation. (e) Reflectance measurement of normal cloth and AgNW-cloth performed by an FTIR microscope using gold film for reference. The collecting angle range of the objective lens is 16°−35.5°. (f) Illustration of the FTIR objective lens. The random scattering of AgNW-cloth and the finite collection angles of the lens limit the measured reflectance.

approximately 86°, 82°, and 78° for 200, 400, and 600 nm spacing, respectively. This high reflectance throughout wide angular range strongly supports the use of metallic nanowire mesh for personal thermal management. When the incident angle reaches 90°, the infrared light with electrical field parallel-polarized to the wire mesh plane has 100% of reflectance, while perpendicular polarization has zero reflectance, making the total reflectance 50%. Besides the analytical simulation, Fourier-transformed IR measurements also show the great reflectance of AgNW-cloth (Figure 2e). The reflectance spectrum of AgNW-cloth and normal cloth is measured from 2 to 15 μm. As expected, the spectrum is nearly flat, with only a slight increase as the wavelength lengthens. The average weighted by human body radiation is 40.8% for AgNW-cloth versus only 1.3% for normal cloth. Here, the IR objective lens covers angles ranging from 16°−35.5° rather than the whole hemisphere; therefore, the discrepancy between experimental and simulation results is due to diffuse scattering and the wavy surface of textiles, as shown in Figure 2f. Nevertheless, the dramatic improvement in IR reflectance clearly indicates that AgNW-cloth is an effective IR reflector and, therefore, suitable for personal thermal management.

The Stefan−Boltzmann law describes thermal emission of objects. For realistic objects, the emissivity (ε) needs to be included as follows:

$$j = \varepsilon\sigma T^4 \quad (1)$$

Where j is the total energy flux, ε is the material emissivity, σ is Stefan−Boltzmann constant, and T is the temperature. At the same temperature, low-emissivity materials radiate less than high-emissivity materials, so they provide more radiation insulation. The emissivity of bulk silver is ~0.02,[27] and common textile is ~0.8, so the overall emissivity of AgNW-cloth is much less than that of normal cloth and provides great insulation against radiative heat loss. Figure 3a−c are thermal images of a human hand with normal cloth, CNT-cloth, and AgNW-cloth, respectively. All samples are in thermal equilibrium with the palm before imaging. For normal cloth and CNT-cloth, the textiles emit IR as detected by the camera. The measured temperature was 33−34 °C. This continuous absorption and emission of IR from human body into the ambient air is a major portion of the heat loss. In contrast, the IR camera shows the AgNW-cloth in the palm as "cold", 30−31 °C. Although the AgNW-cloth has the same temperature as

dx.doi.org/10.1021/nl5036572 | Nano Lett. XXXX, XXX, XXX−XXX

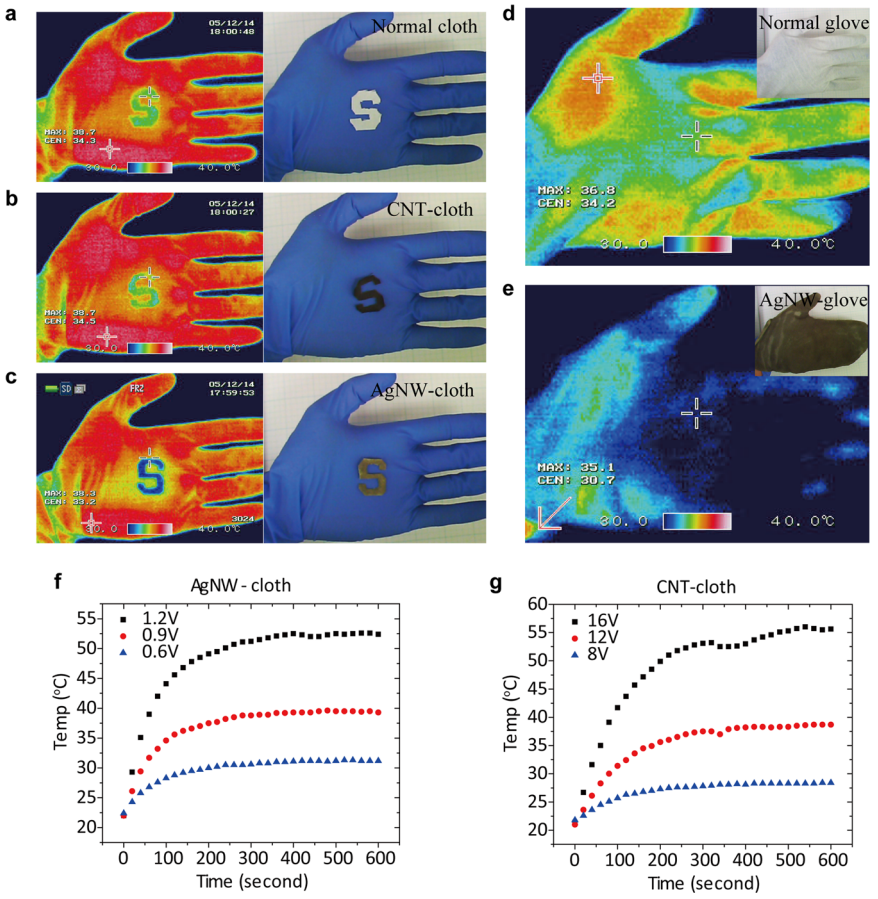

Figure 3. Thermal images (left) and regular photos (right) of normal cloth (a), CNT-cloth (b), and AgNW-cloth (c). The cloth was cut into an S shape and placed in the palm. Only AgNW-cloth is able to block the human-radiated IR and shows the cold color. (d)(e) Side-by-side comparison of thermal images of a human hand with a normal glove and with an AgNW glove, proving the scalability and effectiveness of the dip-coated AgNW-cloth. (f)(g) Temperature change versus time after applying different voltage to a 1 in. × 1 in. sample of AgNW-cloth and CNT-cloth, respectively.

other samples, the low-emissivity and the low thermal radiation of AgNW coating makes the AgNW-cloth appear "cold" in the thermal image. In Figure 3d and e, a normal glove was compared with a full-size AgNW-glove made by the same dip-coating process. The temperature of normal glove ranges from 32 to 37 °C. For the AgNW-glove, most of the thermal radiation from the hand is reflected, and it appears "cold" dark blue color, with a temperature range of 30−34 °C. This demonstrates the scalability and effectiveness of the method of using AgNW solution for the metallic nanowire coating on textiles.

The heat transfer property of normal cloth and AgNW-cloth was compared using an open-air hot plate method (Supporting Information Figure S1). First, the hot plate was covered by a normal cloth to create an air gap between the sample and the hot plate. AgNWs have a higher thermal conductivity than cotton fibers, so the air gap is critical to prevent heat loss from conduction. The temperature of this underlying cloth is set at 31.65 °C to simulate the human body temperature. The sample is then placed on top of the underlying cloth. The more the temperature drops, the better the thermal insulation. Normal cloth has a 4.3 °C temperature drop, whereas AgNW-cloth has 5.2 °C. This means the AgNW coating provide 21% more thermal insulation, which is mainly due to the reduction of radiation loss.

Personal thermal management is not only capable of passive heat trapping but also active warming up. The conducting network of AgNW and CNT cloth fit this purpose perfectly.[28,29] Figure 3f and g show the temperature change versus time when AgNW-cloth and CNT-cloth are applied with voltage. The temperature was measured by a thermal couple in close contact with a 1 in. × 1 in. sample. Because Joule heating is inversely proportional to resistance, AgNW-cloth requires much less voltage to reach the same temperature. For AgNW-cloth, only 0.9 V can induce a temperature change up to 38 °C, higher than human body core temperature 37 °C and skin temperature 33 °C. Although CNT-cloth needs 12 V to reach a similar degree of Joule heating, the energy required to heat up the human body for AgNW-cloth and CNT-cloth are essentially the same, because the electrical energy input equals the thermal energy output. The function of Joule heating further complements the high radiation insulation described previously. It is worth noting that the low voltage required for Joule heating should not pose safety threat to the human body, because the human skin resistance is on the order of 10 000 Ω, much larger than AgNW-cloth and CNT-cloth. In practice, even if an electrical insulation layer is used and decreases the surface temperature (longer wavelength), the IR reflecting property will not be affected, as shown previously in Figure 2b.

After evaluating both the radiation insulating property and the Joule heating function, the question of how much power can be saved by wearing the nanowire cloth must be considered. We assume the condition that includes the outdoor temperature, the dimensions and insulation properties (R_i and

dx.doi.org/10.1021/nl5036572 | Nano Lett. XXXX, XXX, XXX−XXX

ε_i) of the building, the power usage (P_{input}) inside the building, and the insulation properties of normal and nanowire cloths. A detailed description of the calculation can be found in the Supporting Information. The power used by appliances and human beings heat up the building, and the temperature difference causes heat flow to the outside. Depending on how insulating the walls and windows are, the steady-state temperature between inside and outside can be calculated using the following equations

$$P_{input} = P_{loss} = P_{loss}^{conductive} + P_{loss}^{radiative} \quad (2)$$

$$P_{loss}^{conduct} = \sum_i \frac{T_{in} - T_{out}}{R_i A_i} \quad (3)$$

$$P_{loss}^{radiate} = \sum_i \varepsilon_i A_i \sigma (T_{in}^4 - T_{out}^4) \quad (4)$$

Based on our assumed scenario, the outdoor temperature is 10 °C and the indoor temperature is approximately 18 °C. Human skin temperature is generally 33 °C, so the heat loss from the human body into the indoor environment can be deduced using the same equations. The human body's heat loss is 187 W, in which conduction and convection make up approximately 24 W, whereas radiation accounts for as high as 163 W. This is again attributed to the high emissivity of normal cloth, which provides very low radiation insulation. Next, we consider the case of AgNW-cloth with 12 W of Joule heating per cloth. Because of the use of heating AgNW-cloth, the indoor temperature rises slightly. However, it is the reduction of radiation heat loss that plays the major role in reducing human body heat loss from 187 to 96 W and makes the wearer feel warm. We then calculated the required indoor temperature and heater power consumption to induce the same wattage of human body heat loss without wearing AgNW-cloths. The required temperature is 25.5 °C. It takes 366.7 W/person of heater power input to keep this indoor temperature (see Table 1 for a summary). The difference, 366.7 W − 12 W = 354.7 W/person, is the power saved per person by wearing AgNW-clothes. This extent of power saving amounts to 8.5 kWh of heating energy per day per person or ∼1000 kWh per year per person, assuming that heating systems operate for four months a year. If one wanted to offset this power consumption via solar cells, then a 2-m^2-size solar panel would be required per person. For people working in high-rise buildings, it is virtually impossible to allocate a 2-m^2 solar panel for every individual, not to mention the maintenance and installation cost. From this heat loss analysis, one can conclude that AgNW-cloth and personal thermal management is equally competent at alleviating the heavy energy usage today as compared with renewable energy generation.

Table 1. Summary of Power Input and Heat Loss Analysis

	normal cloth only	AgNW cloth only	normal cloth + heater
outdoor temp (°C)	10.00	10.00	10.00
indoor temp (°C)	17.99	18.23	25.55
body heat loss (W/person)	187.3	96.08	96.08
power needed (W/person)	0	12	366.7

Other than operating performance, a personal thermal management device should not sacrifice breathability. When human skin perspires, the nanowire-coated cloth must not prevent the humid vapor from escaping. Otherwise, it would be extremely uncomfortable to wear. For instance, an aluminized Mylar blanket is well-known for its ability to retain body heat by blocking both convective and radiative loss. However, the plastic sheet and the aluminum film are not vapor permeable, so it is not suitable for daily use. In contrast, considering the thin coating and huge spacing (300 nm) of the nanowires vs the size of water vapor molecule (0.2 nm), it is expected that the coating will not affect the breathability. As shown in Figure 4a, we tested the mass increase of desiccant sealed with three types of cloth: normal cloth, AgNW-cloth, and CNT-cloth. All three samples were tested during the same period of time and under the same environment. The fitted slopes represent the breathability, that is, the ability of water vapor to permeate through the cloth and be absorbed by the desiccant. The results show that the coating reduces the breathability only by 2% and 4.6% for AgNWs and CNTs, respectively. All in all, the nanowire coating equips normal cloth with great thermal insulation and active heating ability but still maintains its soft and porous nature to ensure it is still comfortable to wear.

These nanowire cloths are also highly durable against wash cycles. Previous reports have shown that both CNT and AgNWs have excellent adhesion with porous interconnecting substrates because of entanglement with microfibers as well as the surface functionality.[30−32] To investigate the adhesion durability of nanowire cloth, electrical resistance was used to quantify the change of quality of nanowire cloth before and after being washed in swirling clean water, as shown in Figure 4b. Each measurement was conducted after the samples were dried. Surprisingly, for both AgNWs and CNTs, the electrical resistance decreased rather than increasing after the first two washing cycles. This might be due to the removal of unwanted surfactant and increase of packing density after water evaporates from the samples. Starting from the third washing cycle, the resistance remained stable for the following wash cycles, clearly showing the high durability of the nanowire cloths. Besides high durability, the antibacterial properties of AgNWs can also avoid degradation by bacteria and lengthen the lifespan of the personal thermal management cloth (Supporting Information Figure S2).

It is worthwhile to note that only a small amount of AgNWs is required to achieve a highly IR-reflective textile. As shown in Figure 2, considering a single-layer AgNW network, which is 70 nm in diameter, 500 nm in nanowire spacing, and 95% of IR reflectance, the required AgNW mass loading is as low as 0.1 g/m^2. In practice, the quality of connection between each AgNW could influence the IR reflectance. Besides the low mass loading requirement, it would be even more cost-effective to replace AgNW with other metallic nanowire network, for example, copper, nickel, or aluminum.[33−38] The IR properties of these metal nanowires should be very similar to AgNW due to their high electrical conductivity. The oxidation issue of these nonprecious metals can be avoided by proper passivation methods, allowing for both low cost and high durability.[39−41] Other air-stable conducting nanowires, such as metal oxides[42−46] and metal nitrides,[47] can also be applied to the low-emissivity nanowire cloth, provided high carrier concentration and mobility.

In conclusion, through simulation and experiment, we have demonstrated that dip-coated AgNW-cloth has a significantly

dx.doi.org/10.1021/nl5036572 | Nano Lett. XXXX, XXX, XXX−XXX

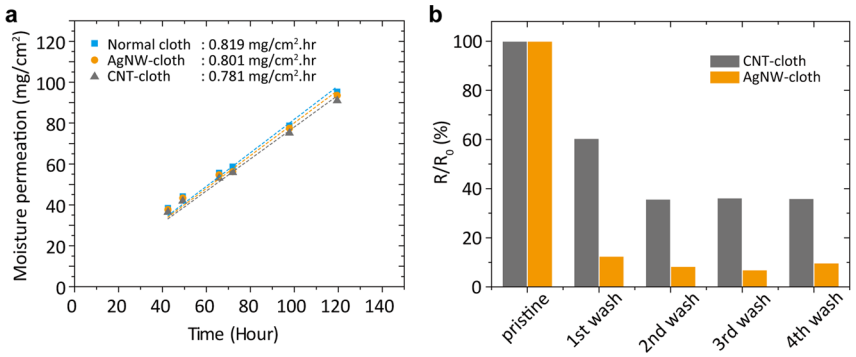

Figure 4. (a) Mass increase of desiccants sealed by the cloth samples. After fitting the data points with linear equation, the breathability is expressed by the slopes. (b) Change of resistance after several wash tests on AgNW-cloth and CNT-cloth. The resistance decreases during the first 2 cycles and then stabilizes without further decay.

higher IR reflectance as well as thermal insulation capability over normal cloth. Both AgNWs and CNTs are capable of performing Joule heating for extra warmth. Moreover, these nanowire coatings maintain the same breathability and durability as normal cloth. Calculations demonstrate this localized-heating nanowire cloth can reduce the power demand by hundreds of watts per person and lessen our dependence on fossil fuel. These promising results exemplify the core value of personal thermal management and provide an important part of the solution for global energy and climate issue.

Method. *AgNW-Cloth Preparation.* A mixture of 0.334 g of polyvinylpyrrolidone (PVP, M.W. = 1 300 000, Sigma-Aldrich) and 20 mL of ethylene glycol (Sigma-Aldrich) was heated at 170 °C in a three-neck glass flask, and then 0.025 g of silver chloride (Sigma-Aldrich) was finely ground and added to the flask for initial nucleation of the silver seeds. After 3 min, 0.110 g of silver nitrate (Sigma-Aldrich), the actual silver source, was titrated for 10 min, followed by an additional 30 min of heating for completion of the reaction. The solution was then cooled down and centrifuged three times at 6000 rpm for 30 min to remove ethylene glycol, PVP, and other impurities in the supernatant. After the final centrifuge, the precipitates of AgNWs were redispersed in 30 mL of isopropanol. Cotton cloth was then dip-coated with AgNW dispersion and vacuum-dried. The mass loading was about 0.6 mg/cm^2.

CNT-Cloth Preparation. Single-walled carbon nanotubes (P3-SWNT, Carbon Solution) were dispersed into 1 wt % of soldium dodecylbenzenesulfonate (SDBS) aqueous solution. The concentration of CNTs was 0.1 mg/mL. The CNT solution was bath-sonicated for 5 min, followed by 30 min of probe sonication. Cotton cloth was then dip-coated with CNT solution and vacuum-dried. The mass loading was 2.9 mg/cm^2

Characterization. FEI XL 30 Sirion Scanning electron microscope was used to characterize the morphology of samples. The operation voltage was 5 kV.

Fourier Transform Infrared (FTIR) Spectroscopy. Spectra were measured using a Nicolet 6700 interferometer coupled to a Continuum XL microscope (Thermo Electron Corp.). IR source light was focused by a 15× objective with angle range from 16° to 35.5°. A variable knife-edge aperture located within the image plane is used to define the sample collection area, which is fixed in size to 200 μm × 200 μm. Spectral range was 650−6000 cm^{-1} with a resolution of 4 cm^{-1}. All spectra are the average of 32 scans at room temperature. The reflectance spectra were plotted as $(R_{sample}/R_{background}) \times 100\%$, where $R_{background}$ was collected from Au film as total reflection mirror.

Thermal Imaging. All thermal images were taken by Mikron thermal imager. The working distance was approximately 30 cm.

Joule Heating Measurement. Nanowire cloth samples were cut into a 1 in. × 1 in. shape, and two adhesive copper tapes were attached on each end of the sample for electrical contacts. The voltage was supplied by a Keithley 2400 SourceMeter, and the sample temperature was monitored by a thermal couple (Watlow), which connects to a temperature controller (Digi-Sense).

Breathability Test. A total of 200 g of desiccant (98% $CaSO_4$ + 2% $CoCl_2$, DRIERITE) was dried in a vacuum oven at 110 °C and then placed into a 250 mL glass media bottle with open-top cap (Fisher). The bottle was then sealed by the cloth sample. The total mass was weighed and recorded periodically. To avoid the bias caused by ambient temperature and humidity, all samples were tested in the same time period.

Wash Test. The nanowire cloths were hung and immersed into swirling distilled water. The water was stirred by a magnetic bar with rotational speed of 600 rpm.

■ ASSOCIATED CONTENT

Ⓢ Supporting Information

Details of simulation model, heat loss analysis model, heat transfer measurement, antibiotic test, and dye test are given in this section. This material is available free of charge via the Internet at http://pubs.acs.org.

■ AUTHOR INFORMATION

Corresponding Author

*E-mail: yicui@stanford.edu.

Author Contributions

P.-C.H. and Y.C. conceived the idea and designed the experiments. P.-C.H. prepared the nanowire cloth and conducted the optical simulation, thermal imaging, Joule heating test, breathability test, and wash cycle test. X.L. conducted the FTIR reflectance measurement. C.L. conducted the antibacterial test. X.X. synthesized the CNT ink. H.R.L. synthesized AgNW ink. A.J.W. conducted the SEM characterization. P.-C.H. and T.Z. conducted the energy saving analysis. P.-C.H. and Y.C. cowrote the paper.

Notes

The authors declare no competing financial interest.

dx.doi.org/10.1021/nl5036572 | *Nano Lett.* XXXX, XXX, XXX−XXX

■ ACKNOWLEDGMENTS

We thank Mr. Alexander Antaris and Prof. Hongjie Dai for providing the IR camera.

■ REFERENCES

(1) Berna, F.; Goldberg, P.; Horwitz, L. K.; Brink, J.; Holt, S.; Bamford, M.; Chazan, M. *Proc. Natl. Acad. Sci. U.S.A.* **2012**, *109* (20), E1215−E1220.
(2) Beerepoot, M.; Marmion, A. *Policies for Renewable Heat: An integrated approach*; OECD Publishing: Paris, 2012; p 9.
(3) Hansen, J.; Ruedy, R.; Sato, M.; Lo, K. *Rev. Geophys.* **2010**, *48*, RG4004.
(4) Metz, B.; Davidson, O. R.; Bosch, P. R.; Dave, R.; L.A, M. *Climate Change 2007: Mitigation of Climate Change*; IPCC: Geneva, 2007; p 863.
(5) Sawin, J. L. *Renewables 2012 Global Status Report*; REN21: Paris, 2012.
(6) *Buildings Energy Data Book*; U.S. Dept. of Energy: Washington, DC, 2011.
(7) *Energy Standard for Buildings Except Low-Rise Residential Buildings*; ASHRAE Standard Committee: Atlanta, GA.
(8) Jelle, B. P.; Hynd, A.; Gustavsen, A.; Arasteh, D.; Goudey, H.; Hart, R. *Sol. Energy Mater. Sol. C* **2012**, *96* (1), 1−28.
(9) Kaushika, N. D.; Sumathy, K. *Renew. Sust. Energy Rev.* **2003**, *7* (4), 317−351.
(10) Gustavsen, A.; Grynning, S.; Arasteh, D.; Jelle, B. P.; Goudey, H. *Energy Buildings* **2011**, *43* (10), 2583−2594.
(11) Sadineni, S. B.; Madala, S.; Boehm, R. F. *Renew. Sust. Energy Rev.* **2011**, *15* (8), 3617−3631.
(12) Sun, Y. G.; Gates, B.; Mayers, B.; Xia, Y. N. *Nano Lett.* **2002**, *2* (2), 165−168.
(13) Chang, Y.; Lye, M. L.; Zeng, H. C. *Langmuir* **2005**, *21* (9), 3746−3748.
(14) Hu, L. B.; Wu, H.; Cui, Y. *MRS Bull.* **2011**, *36* (10), 760−765.
(15) Lee, J. Y.; Connor, S. T.; Cui, Y.; Peumans, P. *Nano Lett.* **2008**, *8* (2), 689−692.
(16) Wu, H.; Hu, L. B.; Rowell, M. W.; Kong, D. S.; Cha, J. J.; McDonough, J. R.; Zhu, J.; Yang, Y. A.; McGehee, M. D.; Cui, Y. *Nano Lett.* **2010**, *10* (10), 4242−4248.
(17) Hsu, P. C.; Wang, S.; Wu, H.; Narasimhan, V. K.; Kong, D. S.; Lee, H. R.; Cui, Y. *Nat. Commun.* **2013**, *4*, 2522.
(18) Hu, L. B.; Kim, H. S.; Lee, J. Y.; Peumans, P.; Cui, Y. *ACS Nano* **2010**, *4* (5), 2955−2963.
(19) Preston, C.; Fang, Z. Q.; Murray, J.; Zhu, H. L.; Dai, J. Q.; Munday, J. N.; Hu, L. B. *J. Mater. Chem. C* **2014**, *2* (7), 1248−1254.
(20) Soltanian, S.; Rahmanian, R.; Gholamkhass, B.; Kiasari, N. M.; Ko, F.; Servati, P. *Adv. Energy Mater.* **2013**, *3* (10), 1332−1337.
(21) Hsu, P. C.; Kong, D.; Wang, S.; Wang, H.; Welch, A. J.; Wu, H.; Cui, Y. *J. Am. Chem. Soc.* **2014**, *136* (30), 10593.
(22) Garnett, E. C.; Cai, W. S.; Cha, J. J.; Mahmood, F.; Connor, S. T.; Christoforo, M. G.; Cui, Y.; McGehee, M. D.; Brongersma, M. L. *Nat. Mater.* **2012**, *11* (3), 241−249.
(23) Lee, T.-W. *Thermal and flow measurements*; CRC Press: Boca Raton, FL, 2008.
(24) Mizuno, K.; Ishii, J.; Kishida, H.; Hayamizu, Y.; Yasuda, S.; Futaba, D. N.; Yumura, M.; Hata, K. *Proc. Natl. Acad. Sci. U.S.A.* **2009**, *106* (15), 6044−6047.
(25) Baughman, R. H.; Zakhidov, A. A.; de Heer, W. A. *Science* **2002**, *297* (5582), 787−792.
(26) Casey, K. F. *IEEE Trans. Electromagn. Compat.* **1988**, *30* (3), 298−306.
(27) *Handbook of Chemistry & Physics*, 95th ed.; CRC Press: Boca Raton, FL, 2014.
(28) Celle, C.; Mayousse, C.; Moreau, E.; Basti, H.; Carella, A.; Simonato, J. P. *Nano Res.* **2012**, *5* (6), 427−433.
(29) Jang, H. S.; Jeon, S. K.; Nahm, S. H. *Carbon* **2011**, *49* (1), 111−116.
(30) Hu, L. B.; Pasta, M.; La Mantia, F.; Cui, L. F.; Jeong, S.; Deshazer, H. D.; Choi, J. W.; Han, S. M.; Cui, Y. *Nano Lett.* **2010**, *10* (2), 708−714.
(31) Schoen, D. T.; Schoen, A. P.; Hu, L. B.; Kim, H. S.; Heilshorn, S. C.; Cui, Y. *Nano Lett.* **2010**, *10* (9), 3628−3632.
(32) Liu, C.; Xie, X.; Zhao, W. T.; Liu, N.; Maraccini, P. A.; Sassoubre, L. M.; Boehm, A. B.; Cui, Y. *Nano Lett.* **2013**, *13* (9), 4288−4293.
(33) Rathmell, A. R.; Wiley, B. J. *Adv. Mater.* **2011**, *23* (41), 4798−4803.
(34) Chen, Z. F.; Rathmell, A. R.; Ye, S. R.; Wilson, A. R.; Wiley, B. J. *Angew. Chem., Int. Ed.* **2013**, *52* (51), 13708−13711.
(35) Ye, S. R.; Rathmell, A. R.; Stewart, I. E.; Ha, Y. C.; Wilson, A. R.; Chen, Z. F.; Wiley, B. J. *Chem. Commun.* **2014**, *50* (20), 2562−2564.
(36) Kawamori, M.; Asai, T.; Shirai, Y.; Yagi, S.; Oishi, M.; Ichitsubo, T.; Matsubara, E. *Nano Lett.* **2014**, *14* (4), 1932−1937.
(37) Fu, M.; Chaudhary, K.; Lange, J. G.; Kim, H. S.; Juarez, J. J.; Lewis, J. A.; Braun, P. V. *Adv. Mater.* **2014**, *26* (11), 1740−1745.
(38) Wu, H.; Kong, D. S.; Ruan, Z. C.; Hsu, P. C.; Wang, S.; Yu, Z. F.; Carney, T. J.; Hu, L. B.; Fan, S. H.; Cui, Y. *Nat. Nanotechnol.* **2013**, *8* (6), 421−425.
(39) Rathmell, A. R.; Nguyen, M.; Chi, M. F.; Wiley, B. J. *Nano Lett.* **2012**, *12* (6), 3193−3199.
(40) Hsu, P. C.; Wu, H.; Carney, T. J.; McDowell, M. T.; Yang, Y.; Garnett, E. C.; Li, M.; Hu, L. B.; Cui, Y. *ACS Nano* **2012**, *6* (6), 5150−5156.
(41) Ahn, Y.; Jeong, Y.; Lee, Y. *ACS Appl. Mater. Interfaces* **2012**, *4* (12), 6410−6414.
(42) Wu, H.; Hu, L. B.; Carney, T.; Ruan, Z. C.; Kong, D. S.; Yu, Z. F.; Yao, Y.; Cha, J. J.; Zhu, J.; Fan, S. H.; Cui, Y. *J. Am. Chem. Soc.* **2011**, *133* (1), 27−29.
(43) Archana, P. S.; Jose, R.; Jin, T. M.; Vijila, C.; Yusoff, M. M.; Ramakrishna, S. *J. Am. Ceram. Soc.* **2010**, *93* (12), 4096−4102.
(44) Lotus, A. F.; Kang, Y. C.; Walker, J. I.; Ramsier, R. D.; Chase, G. G. *Mater. Sci. Eng., B* **2010**, *166* (1), 61−66.
(45) Wan, Q.; Dattoli, E. N.; Lu, W. *Appl. Phys. Lett.* **2007**, *90*, 22.
(46) Wan, Q.; Dattoli, E. N.; Fung, W. Y.; Guo, W.; Chen, Y. B.; Pan, X. Q.; Lu, W. *Nano Lett.* **2006**, *6* (12), 2909−2915.
(47) Li, H. P.; Pan, W.; Zhang, W.; Huang, S. Y.; Wu, H. *Adv. Funct. Mater.* **2013**, *23* (2), 209−214.

dx.doi.org/10.1021/nl5036572 | *Nano Lett.* XXXX, XXX, XXX−XXX